Eur. Phys. J. B **17**, 43–50 (2000)

THE EUROPEAN PHYSICAL JOURNAL B

EDP Sciences

Evidence of domain wall scattering in thin films of granular CoFe-AgCu

V. Franco, X. Batlle, and A. Labarta[a]

Departamento de Física Fundamental, Facultad de Física, Universidad de Barcelona, Diagonal 647, 08028 Barcelona, Spain

Received 30 September 1999

Abstract. Thin films of the giant magnetoresistive granular CoFe-AgCu system prepared by rf sputtering displayed a great variety of domain-like microstructures with a net out-of-plane component of the magnetization for ferromagnetic volume concentrations above about 0.25. Therefore, magnetic percolation takes place at ferromagnetic concentrations much lower than the physical percolation threshold. The out-of-plane structure of the as-deposited samples in magnetic virgin state consisted of a distribution of both quasi-circular domains and short stripes depending on the ferromagnetic content. Furthermore, these samples present high metastability and a variety of remanent in-plane and out-of-plane microstructures can be achieved as a function of the magnetic history. Besides, the evolution of the magnetic microstructure yields strong training effects on magnetotransport properties, due to the extra contribution of the electron scattering at the domain walls. All in all, the observed behavior is the result of a subtle correlation between perpendicular anisotropy produced by residual stresses, exchange interparticle interactions due to CoFe alloyed in the matrix, and dipolar interactions. Thus, as high structural evolution occurs through annealing, the features of randomly distributed ferromagnetic particles are recovered and, the out-of-plane domain structures and the training effects disappear.

PACS. 75.70.Kw Domain structure (including magnetic bubbles) – 75.70.Pa Giant magnetoresistance – 75.60.Lr Magnetic aftereffects

1 Introduction

Nanoscaled structures have generated continuous interest in the past few years. In particular granular alloys, consisting of a distribution of ultrafine ferromagnetic particles dispersed in a non-magnetic metallic matrix, have been widely studied because of their giant magnetoresistance [1,2] (GMR). Besides, many experimental, theoretical and numerical simulation studies have been devoted to the understanding of the in-plane to out-of plane reorientation phenomena of the domain structures observed in thin films [3–9]. These phenomena are a consequence of the balance between perpendicular anisotropy, exchange and magneotostatic energies. These three contributions may be present in granular alloys, thus, these materials also show a wide range of domain-like magnetic microstructures [10]: large in-plane ferromagnetic domains, out-of-plane up and down stripe domains and a variety of intermediate states consisting of a distribution of quasi-spherical domains surrounded by a continuous background of opposite magnetization. Nevertheless, the manner in which that balance takes place is still an open question. It is then of interest to establish both the mechanism responsible for the ferromagnetic interactions among particles and the origin of the perpendicular anisotropy.

[a] e-mail: amilcar@ffn.ub.es

Furthermore, although granular and continuous thin films share similar domain structures, two main differences are worth noting: on the one hand, it is possible in granular alloys to stabilize either in-plane or out-of-plane configurations depending on the magnetic history, while in continuous thin films this reorientation only occurs by varying the film thickness. On the other hand, granular alloys show large metastability, which determines the complex training effects observed in both magnetic and transport properties [11,12].

In this paper, the domain structures appearing in CoFe-AgCu granular alloys below the volume percolation threshold are studied. Special attention has been paid to the dependence of these domain structures on the magnetic history, as well as their contribution to the training effects in magnetotransport properties, associated with the extra contribution to electron scattering at the domain walls [13]. The correlation between the physical microstructure and exchange interactions is also discussed.

2 Experimental

CoFe-AgCu films 200-300 nm thick were rf sputtered onto glass substrates. Fe and Cu were added to the widely studied Co-Ag system, for various reasons: Fe was added

to Co in order to increase the magnetic moment and, consequently, the magnetoresistance effect [14], while a small amount of Cu (about 3% by volume) was added to increase the Co-Ag immiscibility, which leads to a granular system even for as-deposited samples, obviating substrate heating or post-deposition annealing. A variety of samples with ferromagnetic (FM) CoFe concentration, x_v, ranging from 0.10 to 0.40 were prepared. The relative CoFe concentration was 70:30. A detailed description of the experimental procedure is given elsewhere [15]. The composition of the films was determined using energy dispersive X-ray spectrometry (EDX) and inductively coupled plasma mass spectroscopy (ICPMS), with an error less than 2 at.%. The thickness of the films was measured using a multiple-beam interferometer. Post-deposition phase segregation was promoted by rapidly annealing (0.1 s) at 600, 650, 700 and 750 °C. The particle size distribution and the microstructure of the films were studied by X-ray diffraction (XRD) – $\theta/2\theta$ rocking curves and pole figures –, atomic force microscopy (AFM) and transmission electron microscopy (TEM) – bright and dark field, selected area electron diffraction (SAED) and microdiffraction –. Magnetic force microscopy (MFM) was used to image the microscopic pole distribution perpendicular to the film plane. Magnetoresistance (MR) was measured by an ac four point probe technique in the temperature range 4.2–300 K in magnetic fields up to 50 kOe. The relative geometry of the film plane, electrical current and magnetic field was set in three ways: i) the electrical current and the magnetic field were parallel to the film plane (parallel geometry); ii) the in-plane magnetic field was perpendicular to the electrical current (transverse geometry); and iii) H was perpendicular to the film plane (perpendicular geometry). Zero-field-cooled (ZFC) and field-cooled (FC) measurements at low fields were performed with a SQUID magnetometer, in the in-plane geometry. The time dependence of the thermoremanence was measured at various temperatures by field cooling the sample at 50 Oe from room temperature down to the measuring temperature and then switching off the field. Hysteresis loops were measured with a vibrating sample magnetometer, in the in-plane and perpendicular geometries up to 12 kOe.

3 Results

3.1 Structure. Origin of the perpendicular anisotropy

The granular nature of the samples for all the concentrations studied was confirmed by TEM. Both CoFe and Ag crystals have an fcc structure with the $\langle 111 \rangle$ direction textured perpendicular to the film plane. Rocking curves showed that annealing improved texture. Pole figures, $\theta/2\theta$ scans tilting the sample at different angles, and SAED confirmed the $\langle 111 \rangle$ texture. These structural data showed a rhombohedral distortion of the cubic cell: the direction normal to the film plane was squeezed, while the parallel directions were stretched. Low-temperature XRD indicated that this axial deformation grows as temperature decreases due to the different thermal expansion coefficients of the substrate and the film. The positions of the CoFe and Ag peaks were shifted from the bulk values due to the deformation caused by: i) substrate-film stresses associated with differences of the thermal expansion coefficients during deposition; ii) metal alloying; and iii) strains arising from metal coherent interphases. The former is a residual strain that depends on the film thickness and the synthesis conditions, it is observed even for pure as-deposited thin film samples and it is responsible for the axial distortion of the cubic cell. The other two deformations are isotropic. The degree of alloying may be calculated using the Vegard's law leading to a 2% of CoFe diluted in the Ag matrix, for all as-deposited samples independently of x_v. The mean size of CoFe particles is about 3 nm for all as-deposited samples, independently of x_v, which is much larger than those found for as-deposited samples of Co-Ag and CoFe-Ag (see Refs. [14,16]), prepared in similar conditions. Due to the high metastability of the as-deposited samples, a large structural evolution occurs upon annealing. The microstructure evolves to a higher degree of crystallinity: phase segregation and strain relaxation take place, and the crystal symmetry evolves to cubic. The mean size of the particles also increases: the lower x_v, the lower the increase; for example, the mean particle size is about 14(5) nm for $x_v = 0.33(0.10)$ annealed at 750 °C. AFM, TEM, and SAED showed a random distribution of CoFe particles throughout the matrix for as-deposited samples, while during annealing particles coalesce and twins, transparencies and Moiré fringes are observed, suggesting the formation of large particle aggregates. These large aggregates (100 nm) are shown in bright field TEM and AFM, while dark field TEM and XRD yield the real crystal sizes, which are one order of magnitude smaller.

The axial distortion along the $\langle 111 \rangle$ texture direction may be at the origin of the perpendicular anisotropy observed for all the as-deposited samples [17,18]. The value of this uniaxial anisotropy may be found by comparing parallel and perpendicular hysteresis loops [19], yielding values within $0.4–0.5 \times 10^5$ J/m^3 independently of x_v, since all samples have similar thicknesses. The annealing procedure relaxes that stress and the magnetocrystalline anisotropy axis evolves towards the $\langle 100 \rangle$ axis of the cubic cell. Moreover, no columnar growing was observed by cross section TEM in the as-deposited samples.

A detailed study of both the structure and the magnetic anisotropy of this system may be found elsewhere [20].

3.2 Low field susceptibility

The ZFC-FC susceptibility measured at 50 Oe is shown in Figure 1 for the as-deposited samples corresponding to three values of x_v, representative of the overall behavior. For low FM concentrations (*i.e.*, $x_v = 0.12$), the typical features associated with a narrow distribution of small particles are observed. However, the fact that the FC curve is flat below the blocking temperature suggests

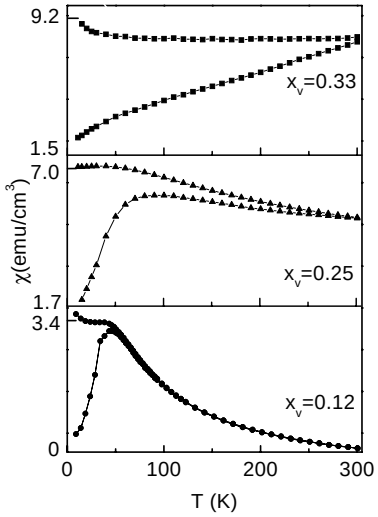

Fig. 1. Zero-field-cooling and field-cooling magnetization as a function of the temperature measured at 50 Oe for $x_v = 0.12$, 0.25, 0.33 as-deposited samples.

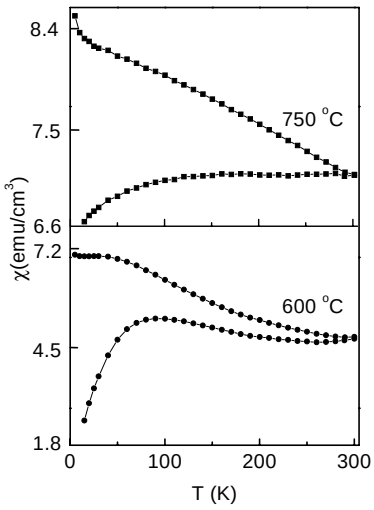

Fig. 2. The same as Figure 1 for $x_v = 0.25$ annealed at 600 °C and 750 °C.

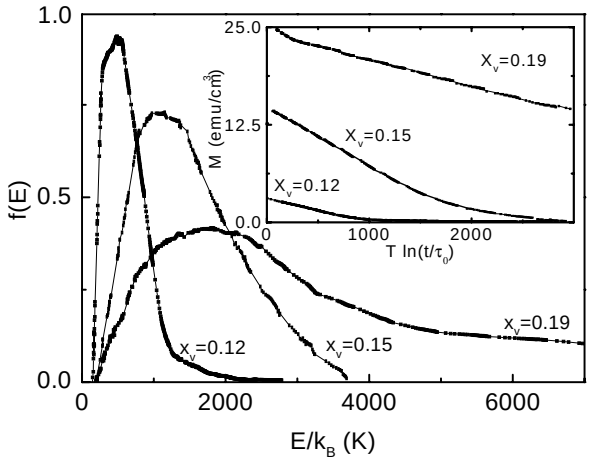

Fig. 3. Effective distribution of energy barriers for $x_v = 0.12$, 0.15, 0.19 as-deposited samples. In the inset, a detail of the $T\ln(t/\tau_0)$ scaling for the same samples, with $\tau_0 = 10^{-11}$ s and temperatures ranging within 5–190 K, is displayed. All relaxation curves were measured in the time window ranging from 1 minute to 1 hour.

some freezing due to interparticle interactions. At intermediate concentrations (*i.e.*, $x_v = 0.25$), the ZFC curve broadens and shifts to higher temperatures; the ZFC and FC curves become progressively temperature-independent above the temperature of the ZFC peak; and the magnetic irreversibility extends up to 300 K. At high concentrations (*i.e.*, $x_v = 0.33$), ZFC-FC display FM-like behavior: the FC curve is almost flat and the ZFC curve increases steadily with temperature as the random distribution of the magnetic moments of the particles is aligned along the field direction. Taking into account that structural data [20] indicate that the mean particle volume, the width of the distribution and the degree of CoFe-matrix alloying is almost independent of the FM concentration, the ZFC-FC curves clearly evidence that magnetic correlations increase with x_v. Thus, although the system is granular for all the concentrations studied (the volume percolation threshold is about 0.50–0.55), magnetic correlations among particles are high enough to induce collective FM behavior above $x_v \simeq 0.25$, when the mean interparticle distance is below *ca.* 1.5 nm. It is worth noting that non-interacting CoFe particles of the given anisotropy energy and mean particle size should be superparamagnetic above *ca.* 10 K (Ref. [21]), which further supports the relevance of interparticle interactions even in those samples with low FM concentration (see Fig. 1 for $x_v = 0.12$).

Through annealing, CoFe segregates completely, while those FM particles surrounded by other FM particles grow, leading to both large magnetic aggregates and isolated particles. At soft annealing there is only a slight increase in the magnetic irreversibility, while the shape of the curves remains the same. In contrast, at high annealing the ZFC susceptibility is almost flat and it is dominated by the large aggregates, while the FC curve steadily increases as temperature decreases and it is dominated by the isolated particles (see Fig. 2).

3.3 Magnetic relaxation

In order to elucidate the role of the CoFe alloyed with the matrix in the appearance of magnetic correlations among particles, the time dependence of the thermoremanent magnetization was analyzed in terms of the $T\ln(t/\tau_0)$ scaling [22]. This scaling yields a single relaxation curve corresponding to the lowest measuring temperature (5 K). The results of this procedure for as-deposited samples with $x_v = 0.12$, 0.15, 0.19 are shown in the inset of Figure 3. It is evident from these data that FM correlations increase with increasing x_v, as already suggested by low field susceptibility, which is related only to the decrease in the interparticle distance, since the size distribution of the FM particles is almost x_v-independent. It is then suggested that indirect FM exchange interactions among particles propagate through the matrix, being aided

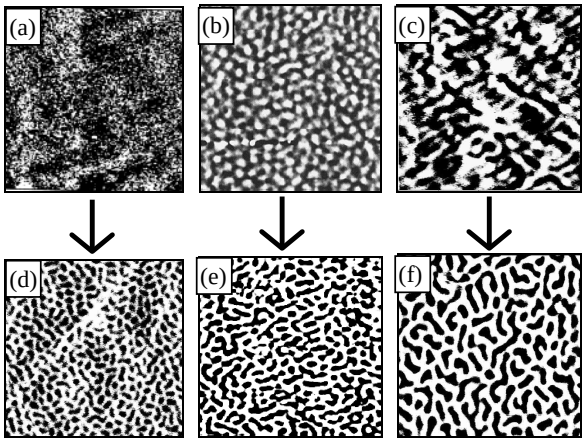

Fig. 4. 5 μm$\times$ 5 μm MFM images of the virgin state for the following as-deposited samples: (a) $x_v = 0.28$, (b) $x_v = 0.33$ and (c) $x_v = 0.40$. 5 μm$\times$ 5 μm MFM images of the remanent state after the application of 10 kOe perpendicular to the film plane for the same as-deposited samples: (d) $x_v = 0.28$, (e) $x_v = 0.33$ and (f) $x_v = 0.40$.

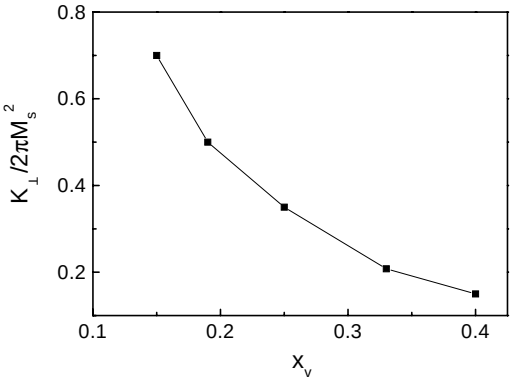

Fig. 5. Ratio of the perpendicular anisotropy to magnetostatic energies as a function of x_v for as-deposited samples.

by the CoFe diluted in the matrix. This conclusion is further supported by the effective distribution of energy barriers, obtained from the time logarithmic derivative of the scaled curves [23], which are shown in Figure 3. These distributions broaden and shift to higher energies as x_v increases, which can be explained by the progressive development of FM exchange interactions, instead of being attributed to dipolar interparticle interactions since the latter are overall demagnetizing for a random distribution of fine FM particles.

3.4 Magnetic force microscopy

In this section, the study of the magnetic microstructure at room temperature by MFM as a function of both the FM content and magnetic history is discussed. Below *ca.* $x_v = 0.25$, the MFM images do not show any additional contrast with respect to the AFM images, indicating that no long-range domain structure with an out-of-plane component is formed. However, for $x_v > 0.25$ a large variety of domain-like structures with a net out-of-plane component of the magnetization arranged in an up and down manner are observed. That concentration is the same at which the low field susceptibility data indicate that magnetic correlations develop throughout the whole system, even at room temperature.

The MFM images corresponding to the as-deposited samples for $x_v = 0.28$, 0.33, 0.40 are shown in Figure 4. No external field was applied to the samples previous to recording the images labeled as (a), (b) and (c) in Figure 4 (virgin state). A well defined up and down domain structure develops with increasing x_v: i) for $x_v = 0.28$, the out-of-plane component is very weak but an alternate magnetic orientation is already evident (Fig. 4a); ii) for $x_v = 0.33$ the MFM signal is larger and corresponds to a distribution of both quasi-circular domains and short stripes (typical size of 200 nm) of the same magnetic polarity, surrounded by a quasi-continuous background of opposite magnetization (Fig. 4b). The smooth transition between black and white regions (grey areas) corresponds to large reorientation domain walls; iii) for $x_v = 0.40$, the domain structure is better defined with sharp transitions between up and down regions (see Fig. 4c). As x_v increases, magnetic domains evolve progressively from an in-plane to an out-of-plane structure with increasing length of the striped domains. The latter is consistent with the energy argument that compares the perpendicular anisotropy and the magnetostatic energies [6]: if $K_\perp/2\pi M_s^2 > 1$, where $K_\perp$ is the perpendicular anisotropy and M_s is the saturation magnetization, a bubble structure appears, while if this ratio is less than one, the stable structure is a striped one. In our case, this value is always less than one and decreases monotonically with x_v (Fig. 5), increasing the stability of the stripe domain structure (see Fig. 4b and 4c).

The domain structures observed in the virgin state can be strongly modified by magnetic history, reaching a great variety of long-life remanent states depending on the magnetic processes previously followed by the sample. Even for the sample with $x_v = 0.28$, for which the virgin state corresponds to most of the magnetization lying in the film plane, the application of a magnetic field of 10 kOe perpendicular to the film plane leads to a stripe-like domain structure, after removing the external applied field (Fig. 4d). The MFM signal increases by a factor 5 in this remanent state with respect to the virgin one. This characteristic remanent state with a striped structure is attained for the whole range of FM concentrations studied above $x_v = 0.25$, whenever the latter magnetization process is carried out (see Figs. 4e and 4f). The MFM signal and the width of the stripes increase with x_v. The mean width is about 100 nm, 120 nm and 140 nm, for $x_v = 0.28$, 0.33, 0.40, respectively, suggesting the increase in the FM correlations. The contrast between up and down domains improves, suggesting that the magnetization is almost out-of-plane in the core of the domains and that the domain walls become narrower. No preferential orientation of the elongated domains is observed since the magnetic field has

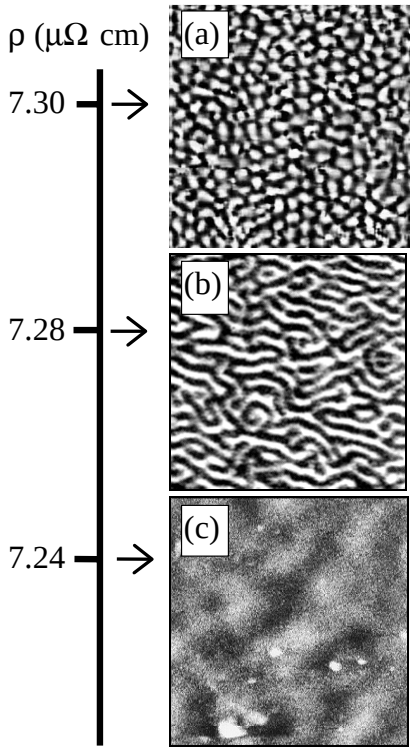

Fig. 6. 5 μm$\times$ 5 μm MFM images of remanent states after different magnetic processes for $x_{\rm v} = 0.33$ as-deposited sample: (a) virgin state; (b) after cycling a field of 10 kOe perpendicular to the film plane; (c) after cycling 10 kOe parallel to the film plane. The values of the resistivity corresponding to these remanent states are also given.

been applied perpendicular to the film plane. After perpendicular demagnetizing cycles are performed (maximum field of 10 kOe) elongated domains coalesce due to domain wall motion and labyrinthine stripe domains some microns long are formed (Fig. 6b). In contrast, parallel demagnetizing cycles largely reduce the out-of-plane component of the magnetization and big shapeless FM in-plane domains of about 1 micron are observed (Fig. 6c). This structure is metastable and slowly evolves to the virgin state (Fig. 6a) (in about 1 month), while the out-of-plane configurations seem to be stable for much longer periods (over one year). The MFM signal (see scan lines in Ref. [11]) increases about two orders of magnitude when going from the remanent state after in-plane saturation (Fig. 6c) to the remanent state after out-of-plane saturation (Fig. 6b) – the maximum deflection angle of the cantilever increases from 0.1° to 7.5° –. Moreover, when the magnetisation of the tip is inverted, the negative of those MFM images with strong signal is obtained (black and white regions are clearly exchanged). All these facts support our assumption that Figure 6b images an out-of-plane domain structure rather than a field gradient associated with the domain walls of a magnetic structure lying mostly in-plane. On the contrary, in those images that we attribute to in-plane domains, the amplitude of the noise is not much lower than the signal itself.

Consequently, in discontinuous granular alloys it is possible to reach those remanent states with a domain structure either in-plane or out-of-plane depending on magnetic history, which is not the case for continuous thin film samples, in which, at the present film thickness (200–300 nm), a striped structure of similar width to the present case is always obtained [3]. A more detailed study of the dependence of the remanent states on the magnetic history for $x_{\rm v} = 0.33$ may be found in reference [12].

The annealing process rapidly reduces the out-of-plane component of the domain structure, leading to large in-plane FM domains at high annealing, as a consequence of the particle clustering shown by TEM and AFM. However, even soft annealing that only slightly modifies the ZFC-FC curves (Figs. 1 and 2) produces a large decay in the MFM signal, which is tentatively attributed to the rapid segregation of the CoFe alloyed with the matrix and to the consequent decrease in the indirect FM exchange interactions through the matrix among CoFe particles.

3.5 Transport properties. Training behavior

The great variety of magnetic microstructures and the associated metastable effects observed in these granular media cause complex transport behavior due to the scattering processes at the domain walls, which leads to strong training effects: transport and magnetic properties evolve with magnetic history. These training phenomena are even detected at low $x_{\rm v}$ contents ($x_{\rm v} \gtrsim 0.15$), where the magnetic interactions are weak and the system displays classical GMR, and become the determinant factor of the magneto-transport properties for concentrations above $x_{\rm v} \simeq 0.30$, when long range correlations develop. These effects are observed only for as-deposited samples, in agreement with the disappearance of the domain structure in the annealed samples.

The dependence of the transport properties on the magnetic history for as-deposited samples with $0.3 < x_{\rm v} < 0.5$ was investigated. In these experiments, MR was measured in the parallel, transverse and perpendicular geometries. The MR loops have a different shape depending on the current field geometry, but a double peak structure is always observed (Fig. 7) due to bimodal behavior, which is related to the in-plane and out-of plane contributions of the domain microstructure to the magnetization [10]. The inner peaks correspond to all the irreversible contributions, such as domain wall motion and those arising from granularity (isolated FM particles and uncompensated moments of the antiparallel arrangement), while the outer broad maxima are attributed to the progressive rotation of the out-of-plane component of the stripe structure towards the field axis. There is also a third contribution at intermediate fields arising from the CoFe alloyed in the matrix, giving place to an anisotropic magnetoresistance (AMR), which is responsible for the slight increase in MR at fields of a few hundred Oe in the parallel geometry (Fig. 7a). There is thus a complex interplay between: i) the GMR contribution arising from the granularity, which is always negative and dominates at low

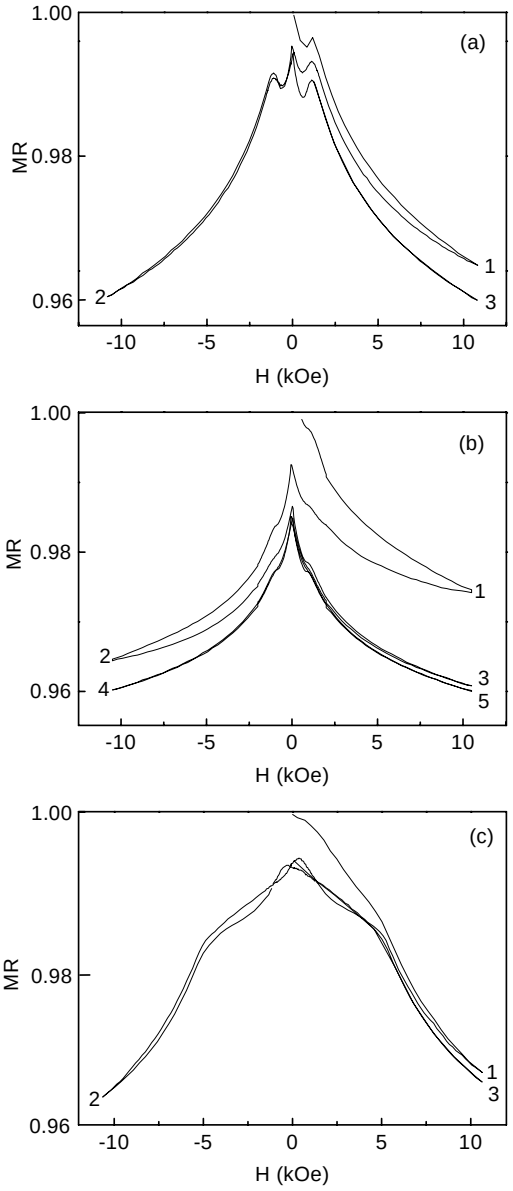

Fig. 7. Repeated cycles of the MR loops at room temperature for $x_v = 0.33$ as-deposited sample originally at the virgin state, measured in three different geometries: (a) parallel; (b) transversal and (c) perpendicular. The numbers indicate the sequence in which the data have been recorded.

fields; ii) the AMR contribution, which is positive in the parallel geometry and negative in transversal and perpendicular ones, and which is relevant at intermediate fields; iii) the MR contribution coming from the scattering at the domain walls [13], which is also negative in all geometries and significatively contributes at fields above 1 kOe.

This overall behavior is consistent with the main features of the corresponding hysteresis loops: the inner peaks occur at the coercive field (about 100 Oe) and the outer peaks occur at the field at which irreversibility disappears [10,24]. Both the hysteresis loops and the MR curves for annealed samples display the typical features of a distribution of FM particles, showing classical GMR, and no bimodal behavior [1,2].

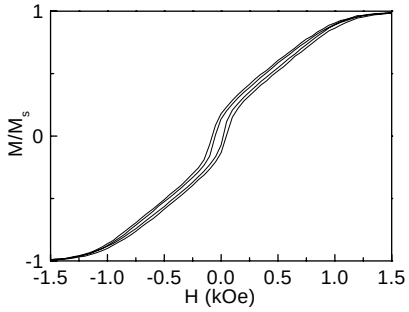

Fig. 8. Two complete cycles of the hysteresis loop of the magnetization at room temperature for $x_v = 0.33$ as-deposited sample originally at the virgin state.

An example of the training behavior starting from the virgin state is shown in Figure 7 for the as-deposited sample with $x_v = 0.33$ at room temperature for the three geometries. The difference in the shape of the curves in the parallel and perpendicular geometry is a direct consequence of the demagnetizing field and the change in sign of the AMR contribution. In the transversal geometry, the outer peaks are flattened with respect to the parallel geometry because AMR is negative. By cycling an in-plane field of 10 kOe in the parallel and transversal geometries (Figs. 7a and 7b), the magnetic order of the system increases due to the reduction in the total surface of the domain walls (larger domains sizes); consequently, the resistance of the system is reduced. After a certain number of cycles (3-9) the system is trapped in a long live metastable state and training effects disappear. After 24 hours at zero field a similar state to the original one is recovered and the training behavior may be reproduced. However, by cycling a magnetic field of 10 kOe perpendicular to the film plane (Fig. 7c), smaller training effects are observed, and a more stable state than that corresponding to the virgin one is rapidly achieved. Training effects are no longer observed when magnetic cycles are repeated. These results are consistent with the fact that the MFM images of the remanent state after in-plane magnetic saturation, evolve slowly to the original virgin state, while the MFM images after application of a perpendicular field are the same one year later. In addition, the shapes of the MR curves are slightly modified, smoothed or roughened, by the sweeping rate of the field, so that more cycles are necessary to attain the long life metastable state when the field is swept rapidly.

The hysteresis loops of the virgin samples display similar training behavior. In Figure 8, the hysteresis loops obtained by cycling an in-plane magnetic field twice are shown, suggesting the reduction in the magnetic irreversibility as the domain size increases and the total surface of the domain walls decreases.

A direct evidence of the extra contribution due to the scattering at the domain walls may be gained by measuring the resistivity of the samples at zero field after different magnetic histories that lead to the variety of domain

structures observed by MFM. We show in Figure 6 the MFM images at $H = 0$ for $x_v = 0.33$, in the virgin state and after perpendicular and parallel demagnetizing cycles are performed, also indicating the corresponding values of the resistivity measured in those three remanent states. It is evident from Figure 6 that resistivity decreases as magnetic domains grow and the total surface of the domain walls is reduced. Therefore, the lowest resistivity values are obtained for the remanent states after parallel cycling, in which large and irregular-shaped in-plane domains are present (Fig. 6c), while the highest one is measured in the virgin state (Fig. 6a) for which the mean domain size is much smaller. Intermediate resistivity values are found when a well-defined out-of-plane striped structure is observed after perpendicular cycling (Fig. 6b), because the elongation of the domains along the stripe direction decreases the domain wall contribution, even though the width of the elongated domains is practically unchanged with respect to that observed in the virgin state.

4 Discussion

Similar domain structures to those observed in CoFe-AgCu for $x_v > 0.25$ have been reported in pure Co thin films prepared by different methods [3–6,13]. In those materials with strong perpendicular anisotropy, these domain structures have been attributed to the competition between wall and shape energies. An out-of-plane configuration of the magnetization does not minimize the magnetostatic energy, which tends to keep the magnetic moments in the film plane. However, Kittel [25], based on energy arguments, predicted that for thickness greater than a critical value a reorientation transition from in-plane to out-of-plane would occur. This critical thickness is about 30 nm for pure hcp Co films [3]. Moreover, depending on the thickness of the Co films a diversity of domain structures either in-plane or out-of-plane have been found experimentally: in-plane domains with vortex structure [5,26]; perpendicular stripes [3,27,28]; and complex domain structures with closure domains [28,29]. Similar microstructures have also been found by numerical simulation of a bidimensional Heisenberg system with perpendicular anisotropy and competing dipolar and exchange interactions [8,9,30]. However, the comparison between the experimental results for continuous thin films and the numerical results must be taken as tentative, since the numerical model does not include the domain wall energy along the perpendicular direction.

It is then clear that out-of-plane domain structures will appear in discontinuous granular magnetic films due to the interplay between perpendicular anisotropy and dipolar and exchange interactions.

The origin of the perpendicular anisotropy observed in the as-deposited samples is related to substrate-film stresses produced by the rapid quenching during deposition, as has been reported for a great variety of thin film systems [17]. For example, an axial deformation of about 0.01% of a hexagonal cell is enough to induce dominant magnetoelastic uniaxial anisotropy [18]. In CoFe-AgCu granular alloys, typical values of the deformation of about 0.6% are found [20]. An indirect evidence of the correlation between substrate-film stresses and uniaxial perpendicular anisotropy is the fact that, as soon as annealing relaxes strains, the anisotropy evolves to the $\langle 100 \rangle$ cubic axis.

Long range dipolar interactions are an intrinsic feature of systems constituted by a random distribution of small particles and they are responsible for the magnetostatic energy in continuous media. Granular thin films share both contributions, and their relative importance related to mean interparticle distance, which is monitored by x_v.

In these alloys, FM exchange interactions among particles occur since the size of the domain structures is much larger than the typical size of the CoFe particles. This FM exchange is tentatively attributed to direct exchange through the surface of neighboring particles and indirect exchange through the matrix aided by the 2% of CoFe atoms diluted in the matrix for as-deposited samples. Then, as the FM particle distribution is narrow, the mean size is nearly the same for all as-deposited samples and the degree of alloying is constant with x_v, the mean interparticle distance is reduced by increasing x_v. When it is below about 1.5 nm at $x_v \gtrsim 0.25$, FM interactions are strong enough to develop long range domain-like structures. This degree of alloying is similar to the values reported for other granular alloys [31].

It has been shown that as-deposited samples display large metastability, it being possible to achieve in-plane or out-of plane configurations as a function of magnetic history. However, those remanent states with an out-of plane component of the magnetization seem to be more stable than the virgin states, probably since the latter corresponds to non-equilibrium state due to the rapid quenching during deposition. This metastability is also at the origin of the training behavior observed in magnetotransport properties, through the extra contribution to the electron scattering at the domain walls. Since this metastable behavior is more extreme than in continuous thin films, it is suggested that it may be related to the role of defects, non-epithaxy and grain boundaries, which act as pinning centers. As a consequence, both out-of-plane and in-plane remanent states can be stabilized for a given value of x_v and the film thickness, which is not the case for continuous thin films.

The annealing procedure destroys the out-of-plane configurations and the system behaves as classical FM material, due to the segregation, growing and clustering of the particles, leading to large in-plane domains.

5 Conclusions

Although CoFe-AgCu alloys are granular in nature below the percolation threshold, they show for $x_v > 0.25$ some characteristic features of continuous systems, such as out-of-plane domain-like structures. This indicates that magnetic percolation takes place at concentrations much lower than physical percolation ($x_p = 0.50 - 0.55$). However,

the granularity of the system affects the overall behavior, and for example no discontinuity suggesting the nucleation of magnetic bubbles is observed in the hysteresis loops at high perpendicular fields since domain inversion does not take place continuously, in contrast to Co thin films [3]. Furthermore, the granularity of the system also leads to the training effects observed in both magnetic and transport properties. All these features suggest that granular alloys displaying long-range domain-like structures share some features of both continuous and discontinuous thin films.

Finally, the extra contribution to the magnetoresistance coming from the scattering at the domain walls has been clearly evidenced by studying the resistivity of the samples in a variety of remanent states, and the variations in the resistivity values have been correlated to the domain microstructures observed by MFM. It is thus concluded that the resistivity decreases as the total surface of the domain walls is reduced. As far as we know, this is the first time that this extra contribution to the electron scattering is ascertained in granular systems.

We would like to thank Dr. M.L. Watson for supplying the facilities to synthesize the samples. Financial support of both the Spanish CICYT through the MAT-97-0404 project and the Catalonian CIRIT through the GRU-1012 and SR119 projects are largely recognized. The Spanish-British Joint Action HB 1996-0066 is also acknowledged.

References

1. A.E. Berkowitz, J.R. Michell, M.J. Carey, A.P. Young, S. Zhang, F.E. Spada, F.T. Parker, H. Hutten, G. Thomas, Phys. Rev. Lett. **68**, 3745 (1992)
2. J.Q. Xiao, J.S. Jiang, C.L. Chien, Phys. Rev. Lett. **68**, 3749 (1992).
3. M. Hehn, S. Padovani, K. Oudnajela, J.P. Bucher, Phys. Rev. B **54**, 3428 (1996).
4. M. Hehn, K. Cherifi-Khodjaoui, K. Oudnajela, J.P. Bucher, J. Arabski, J. Magn. Magn. Mater. **165**, 520 (1997).
5. D.M. Donnet, K.M. Krishnan, Y. Yajima, J. Phys. D **28**, 1942 (1995).
6. S. Hamzaoui, M. Labrune, I.B. Puchalska, J. Magn. Magn. Mater. **22**, 69 (1980).
7. S.T. Chui, J. Appl. Phys. **79**, 4951 (1996).
8. L.C. Sampaio, M.P. de Albuquerquer, F.S. de Menezes, Phys. Rev. B **54**, 6465 (1996).
9. A.B. MacIsaac, J.P. Whitehead, K. De'Bell, P.H. Poole, Phys. Rev. Lett. **77**, 739 (1996); A.B. MacIsaac, K. De'Bell, J.P. Whitehead, Phys. Rev. Lett. **80**, 616 (1998).
10. X. Batlle, V. Franco, A. Labarta, M.L. Watson, K. O'Grady, Appl. Phys. Lett. **70**, 132 (1997).
11. V. Franco, X. Batlle, A. Labarta, J. Magn. Magn. Mater. **196-197**, 465 (1999).
12. V. Franco, X. Batlle, A. Valencia, A. Labarta, K. O'Grady, M.L. Watson, K. O'Grady, IEEE Trans. Magn. **34**, 912 (1998).
13. J.F. Gregg, W. Allen, K. Ounadjela, M. Viret, M. Hehn, S.M. Thompson, J.M.D. Coey, Phys. Rev. Lett. **77**, 1580 (1996).
14. S.R. Teixeira, B. Dieny, A. Chamberod, C. Cowache, S. Auffret, P. Auric, J.L. Rouviere, O. Redon, J. Pierre, J. Phys. Cond. Matter **6**, 5545 (1994).
15. F. Badia, X. Batlle, A. Labarta, M.L. Watson, A.B. Johnston, J.N. Chapman, J. Appl. Phys. **82**, 677 (1997).
16. H. Sato, Y. Kobayashi, Y. Aoki, H. Yamamoto, J. Phys. Cond. Matter **7**, 7053 (1995).
17. S. Chikazumi, *Physics of Magnetism* (R.E. Krieger Publishing Co, INC., 1964).
18. C.H. Lee, Hui He, F.J. Lamelas, W. Vavra, C. Uher, R. Clarke, Phys. Rev. B **42**, 1066 (1990).
19. J.Q. Xiao, C.L. Chien, A. Gavrin, J. Appl. Phys. **79**, 5309 (1997).
20. V. Franco, X. Batlle, A. Labarta, J. Bases, F. Sandiumenge, Acta Mater. **47**, 1661 (1999).
21. The temperature of the maximum in the ZFC curve and the mean blocking temperature may be calculated as indicated in: J.I. Gittleman, B. Abeles, S. Bozowski, Phys. Rev. B **9**, 3891 (1974).
22. A. Labarta, O. Iglesias, Ll. Balcells, F. Badia, Phys. Rev. B **48**, 10240 (1993).
23. O. Iglesias, F. Badia, A. Labarta, Ll. Balcells, Z. Phys. B **100**, 173 (1996).
24. V. Franco, X. Batlle, A. Labarta, M.L. Watson, K. O'Grady, J. Appl. Phys. **81**, 4593 (1997).
25. C. Kittel, Phys. Rev. **70**, 965 (1946).
26. R. Allenspach, M. Stampanoni, A. Bischof, Phys. Rev. Lett. **65**, 3344 (1990).
27. P.J. Grundy, D.C. Hothersall, G.A. Jones, B.K. Middleton, R.S. Tebble, Phys. Status Solidi a **9**, 79 (1972).
28. A. Hubert, Physica **22**, 709 (1967).
29. W. Szmaja, K. Polanski, K. Dolecki, J. Magn. Magn. Mater. **151**, 249 (1995).
30. O. Iglesias, A. Valencia, A. Labarta, J. Magn. Magn. Mater. **196-197**, 819 (1999).
31. B. Dieny, S.R. Teixeira, B. Rodmacq, C. Cowache, S. Auffret, O. Redon, J. Pierre, J. Magn. Magn. Mater. **130**, 197 (1994).